THE ANATOMICAL RECORD 256:29–39 (1999)

Anatomical Characteristics and Three-Dimensional Model of the Dog Dorsal Lateral Geniculate Body

INAH LEE, JEJOONG KIM, AND CHOONGKIL LEE*
Department of Psychology, Seoul National University, Kwanak, Seoul 151–742, Korea

ABSTRACT

The morphological and laminar characteristics of the dorsal lateral geniculate nucleus (LGN) and medial interlaminar nucleus (MIN) of the domestic dog (*Canis familiaris*) were studied by three-dimensional computer reconstruction of labeled retinal afferents following intraocular HRP injections. As previously reported, the dog LGN consisted of layers A, A1, C, C1, C2, and C3. Layers A, C, and C2 receive contralateral-eye inputs, and layers A1 and C1 ipsilateral inputs. The dog MIN was found to have four orderly interdigitating layers; layers 1, 2, 3, and 4, medial to lateral. MIN layers 1 and 3 received contralateral inputs, and layers 2 and 4 ipsilateral inputs. Layer 1 had the largest soma of all LGN/MIN layers. LGN layer A was partially separated into medial and lateral subdivisions by a cleft free of somata. The overall three-dimensional shape of the lateral geniculate body was like the letter C, with the convex part of the C directed posteriorly. The relative volume of the MIN was smaller than in the cat; the canine MIN comprised 8.3% of the combined volume of layers A, A1 and the MIN, while that of the cat comprised 14.2% as estimated from Sanderson's map. The volume of all contralateral-eye layers, combining both LGN and MIN, was 31.2 mm^3 (78%), and that for ipsilateral layers was 8.6 mm^3 (22%). The ratio of ipsilateral to contralateral laminar volumes is much lower in the dog than in the cat. Anat Rec 256:29–39, 1999. © 1999 Wiley-Liss, Inc.

Key words: visual system; medial interlaminar nucleus; volumetry; horseradish peroxidase; computer reconstruction; scotopic vision; lateral geniculate

In the domestic cat (*Felis catus*), the medial interlaminar nucleus (MIN), a medial subdivision of the lateral geniculate body (LGB), has a special role in dim-light vision. It almost exclusively represents a region of retina roughly coincident with the reflective tapetum (Lee et al., 1984), and cells of the MIN have relatively high luminance threshold at low adaptation levels (Lee et al., 1992). The MIN has been described in many families of mammalian carnivores (Sanderson, 1974) suggesting that specialization for dim-light vision may be a general function of this structure. However, except for the cat, there is little specific information on functional organization and physiological characteristics of the MIN. As a preliminary step to investigate this relationship in another member of the carnivore family, we examined the laminar pattern of the entire LGB in one domestic dog breed, the *Sapsaree*. Anecdotal evidence suggests that the dog has excellent dim-light vision.

The morphological and cytoarchitectonic features of the domestic dog LGB have been commented on in a few studies. Rioch (1929) identified four layers of the dorsal lateral geniculate nucleus (LGN): lamina principalis anterior, lamina principalis posterior, lamina magnocellularis, and lamina parvocellularis. These layers correspond to layers A, A1, C, and C1–C3 of the cat LGN, respectively. Chadzypanagiotis et al. (1968) described cytoarchitectonic characteristics of the dog LGN, and also mentioned a

Inah Lee's present address is: Department of Psychology, University of Utah, Salt Lake City, Utah 84112.

Grant support: Korea Ministry of Science and Technology.

*Correspondence to: Choongkil Lee, Department of Psychology, Seoul National University, Kwanak, Seoul 151–742, Korea. E-mail: cklee@snu.ac.kr

Received 11 February 1999; Accepted 18 May 1999

© 1999 WILEY-LISS, INC.

group of large cells corresponding to the medial interlaminar nucleus (MIN) of the cat. Morimoto et al. (1984) identified most characteristics of the cat LGB in the dog, describing the dog MIN as having two layers receiving contralateral and ipsilateral retinal afferents.

Our aim was to characterize anatomical features completely enough for guiding subsequent physiological studies. The method we used for determining laminar structure was to three-dimensionally reconstruct labeled retinal afferents following intraocular injection of an anatomical tracer, horseradish peroxidase (HRP). This strategy enabled us to unambiguously determine the subdivisions and layers of the LGB, to view complete three-dimensional features, and to estimate volume of each layer. Confirming previous results, the dog LGB consists of two subdivisions: the lateral geniculate nucleus (LGN) and the medial interlaminar nucleus (MIN). The MIN, however, was found to have more layers than previously thought: four orderly interdigitating layers receiving inputs from the contralateral and ipsilateral eyes.

MATERIALS AND METHODS

Two male dogs, 6 and 12 months old, weighing 10 and 12 kg, were used. The dogs were obtained from a breeding colony maintained by the Foundation for Sapsaree Conservation at Daegu, Korea. The animals were tranquilized with ketamine hydrochloride (5 cc, Ketalar, Yuhan Co.) and xylazine hydrochloride (1 cc, Rompun, Bayer), and 2–3 drops of ophthalmic anesthetic (Proparacaine Hydrochloride 0.5%) applied into the left eye. Then 20 mg of HRP (Sigma) dissolved in 50 μl of saline was injected into the anesthetized eye at its lateral margin (5 mm from limbus). The injection was made over 2–3 min, and the injection needle (26 g) remained inserted for an additional 2–3 min after completion of the injection. An ophthalmic anesthetic was given afterwards. Animals survived 48 hr after the tracer injection. The care and use of animals was in accordance with the guidelines of the Seoul National University Animal Care Advisory Committee, Society for Neuroscience and the National Institute of Health. All efforts were made to minimize animal suffering, and to reduce the number of animals used.

For transcardiac perfusion, animals were first tranquilized with ketamine hydrochloride (5 cc, Ketalar, Yuhan Co.) and xylazine hydrochloride (1 cc, Rompun, Bayer), and then a lethal dose of sodium thiopental (500 mg, ChoongWae Co.) was intravenously injected. The dogs were immediately perfused with 3 liters of buffered saline, followed by 6 liters of Karnovsky's fixative (4% glutaraldehyde and 1% paraformaldehyde in 0.1 M PO_4 at pH 7.4), followed by 6 liters of 10% buffered sucrose (0.1 M PO_4, pH 7.4, 4°C). Immediately after perfusion, the skull was opened and a block containing the LGB (A4–A16.5) from both sides was removed from the brain, using a knife held by a Narishige carrier on a stereotaxic frame to cut the block in standard Horsley-Clarke plane. For alignment purposes, a needle hole and a knife cut groove shaped like a V at the ventral margin of the block, were made anteroposteriorly. The block was stored in 30% sucrose (PO_4, 4°C) for 3–4 days until it sank. Both eyes were removed and stored for drawing retinal landmarks and the boundary of the tapetum.

The block containing the LGB from both sides of the brain was frozen and cut into 17 μm coronal sections with a sliding microtome. Every third section was processed according to the method of Mesulam (1982). Adjacent sections were counterstained with neutral red in addition to being processed for HRP. The final linear shrinkage was estimated to be 18% when both the brain shrinkage after perfusion and the shrunken distance between blood vessels after HRP processing were taken into account. All dimensions for distance and volume in this report are corrected for this shrinkage, unless otherwise stated. A block containing the LGB's of an additional dog (*Sapsaree*) was processed for cresyl violet stain for examining laminar cytoarchitecture.

The boundaries of LGN/MIN zones filled with HRP-labeled retinal afferents were traced under a microscope (Olympus, BX50) with the aid of a drawing tube (final magnification ×32). Light field, dark field, and polarized illumination were used to determine labeled zones and to better delineate these boundaries. Blood vessels appearing across several sections were also drawn and used later for fine alignment. Since the laminar assignment of labeled zones was difficult in serial coronal sections, especially in border zones between the LGN and the MIN, the zones filled with labeled retinal projections were first three-dimensionally reconstructed. For this purpose, the boundaries of labeled zones were drawn for serial sections spaced every 51 μm (every third section), aligned with the aid of blood vessels, and scanned into a computer with a resolution of 600 dpi. Areas with enclosed boundaries were filled in individual images. These filled zones were combined into 3D structures for the sides contralateral and ipsilateral to the HRP injection, using a commercial software package (Voxwin 1.2.2, Voxar Co., U.K.).

When the reconstructed 3D images were examined by rotation, ambiguities in laminar assignment with 2D sections were considerably reduced, and each 3D structure was tentatively assigned to one of the LGN/MIN layers. The labeled zones in the original coronal sections were checked against this laminar assignment, and morphological characteristics of soma in adjacent counterstained sections were noted for each layer. Ambiguities in laminar assignment were resolved by the cytoarchitecture, and the laminar assignments accordingly adjusted in two- and three-dimensional views until any inconsistencies were resolved. As this process was repeated, laminar assignments were updated and optimized, based on morphological and cytoarchitectonic characteristics of the laminar structure. Once the final three-dimensional model of the LGB was derived, two-dimensional images in parasagittal and horizontal series were generated along with corresponding laminar assignments, using the same software package. The volume of each layer was estimated by voxel counts in the model.

For comparison, laminar volumes of the cat were estimated using Figures 9–18 of Sanderson (1971). His Figures 10–18 (nine coronal drawings) were scanned into digital images as described above. As his drawings did not distinguish sublayers within the C layers and those within the MIN, volumes of the C layers and the MIN as a whole were obtained along with volumes of layers A and A1. Anteriormost and posteriormost parts of the LGB beyond the levels shown in his Figures 10 and 18, were extrapolated by areal decrease, the magnitude of which was determined from his Figure 9 (parasagittal drawing).

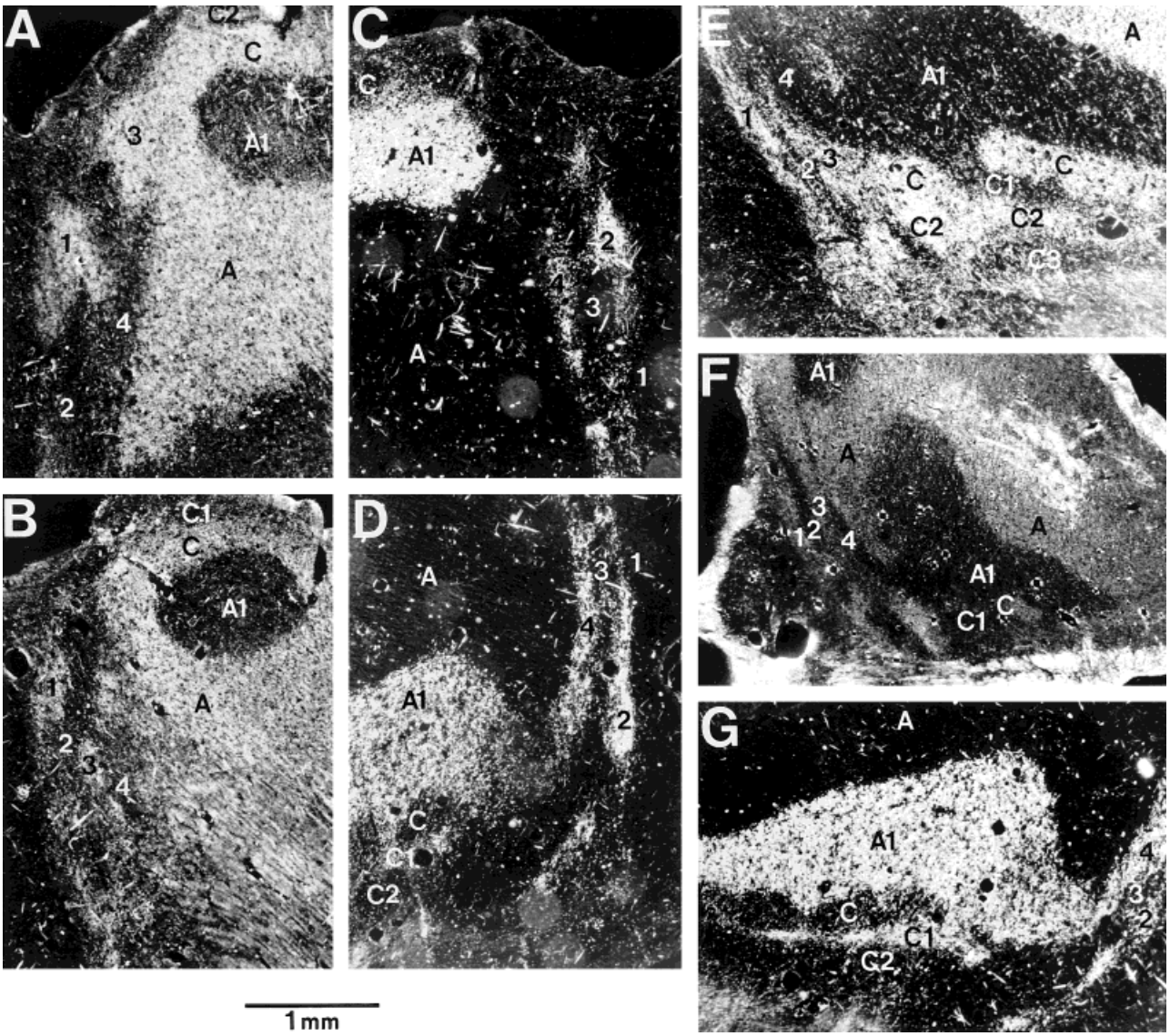

Fig. 1. Composite photomicrographs of representative HRP-reacted coronal sections. All photomicrographs were taken with polarized illumination. Zones filled with labeled retinal afferents appear white. Laminar assignments (A, A1, C, C1, C2 for the LGN and 1, 2, 3, 4 for the MIN) were made in conjunction with the three-dimensional reconstruction. **A:** Dorsal aspect of the contralateral side. MIN layer 1 appears as an inverted V. Layers 3, C, and A merge in this section. These layers, however, were distinguishable by differences in soma size in Nissl-stained adjacent sections. **B:** Contralateral side, more anterior to A. Layer 3 is separated from A and C. MIN layers 1 and 3 are barely visible. **C:** Dorsal aspect of the ipsilateral side. Labeled zones are A1, MIN-2, and MIN-4. The uppermost part of the labeled zone corresponding to layer 2 (zone surrounding the number 2) shows a stronger label. **D:** Ventral aspect of the ipsilateral side. Two MIN layers (2 and 4) are clearly identifiable. Layer 2 extends ventrally further than layer 4. **E:** Ventral aspect of the contralateral side. Layer C is broken by a connected part between A1 and C1, this connected part is labeled in Figure 1D. Weakly labeled in C3 are fibers-of-passage, and C3 is devoid of labeled terminals. As shown by this section, label in C2 is relatively strong. Labeled zone below C3 is the optic tract. Layers C, C2, and MIN-3 merge in this coronal section. **F:** Orderly lamination of the four layers of the MIN can be seen. Magnification of this figure is different from the rest, with the calibration bar corresponding to 2 mm. **G:** Ventral aspect of the ipsilateral side. Layers A1 and C1 fuse.

RESULTS

As outlined above, the dog LGB consists of an LGN and MIN in an arrangement similar to that of other carnivores. The dog MIN, however, has four layers, as will be shown below. We follow and extend the naming scheme that Guillery et al. (1980) used for the cat; layers A, A1, C, C1, C2, and C3 for the LGN, anterior to posterior, and layers 1, 2, 3, and 4 for the MIN, medial to lateral. The results described below are primarily from one animal; unless otherwise mentioned, they were consistent in the other animals.

HRP-Labeled Zones

Serial coronal sections were processed to delineate zones filled with labeled retinal afferents. The assignment of layers relied primarily on the three-dimensional reconstruc-

tion and the morphological characteristics of soma. Figure 1 shows composite photomicrographs of representative HRP-reacted coronal sections, taken with polarized illumination. On the contralateral side, LGN layers A, C, C2 and MIN layers 1 and 3 were filled with labeled retinal afferents (Figs. 1A, B, E, F). On the ipsilateral side, LGN layers A1, C1, and MIN layers 2 and 4 were filled with labeled projections (Figs. 1C, D, G).

A new finding of this study was that the dog MIN is organized into four orderly arranged layers: two contralateral (1 and 3, Fig. 1E) and two ipsilateral (2 and 4, Fig. 1D) forming a regularly interdigitating pattern observable in low magnification (Fig. 1F). In posterior sections, layer 1 looks like an inverted V in this animal, and layers 3, C, and A appear to merge in the HRP-reacted material (Fig. 1A). These layers, however, were distinguishable by soma size in Nissl-stained adjacent sections. In more anterior sections, layer 3 was separated from A and C (Fig. 1B). On the side ipsilateral to the HRP injection, two MIN layers were clearly identified in addition to LGN layers A1 and C1 (Figs. 1C,D). For the initial stage of the analysis, the laminar assignment was ambiguous, and we were particularly concerned with the fourth layer of the MIN, since it had not been previously described. The three-dimensional view indicated that it was unlikely that layer 4 was the continuation of either layer A1 or layer C1 of the LGN. MIN layer 4 continued to be labeled at more anterior level of the LGB than layer 3. Layers 2 and 4 ran dorsoventrally, forming two parallel tiers in coronal sections. The dorsalmost and ventralmost parts of these tiers showed a higher density of labeled afferents and contained larger somata, and were connected by weakly labeled middle parts (Figs. 1C,D). Layer 2 extended further ventrally than layer 4 (Fig. 1D).

A labeled zone corresponding to C1 was narrow and often connected to A1, breaking the continuity of layer C (Figs. 1D, E, G). The density of labeled afferents in C2 was relatively high (Fig. 1E). Layer C3 may be seen, devoid of labeled retinal afferents from either eye in Figure 1E. A retino-recipient zone medial to the MIN, the "geniculate wing," described in the cat (Guillery et al., 1980) was not found in our material.

Computer-Generated Two-Dimensional Sections

Figure 2 shows representative laminar assignments for contralateral (A) and ipsilateral (B) sides of the brain in coronal sections, and for the contralateral side only in parasagittal (D) and horizontal (E) series. All the slices were generated by "cutting" the three-dimensionally reconstructed LGB using the software package. Five contralateral eye layers (layers A, C, C2 for the LGN, and layers 1, 3 for the MIN) and four ipsilateral layers (layers A1, C1 for the LGN, and layers 2, 4 for the MIN) are shown. Layer A is partially divided into medial and lateral parts by a cleft free of somata. This cleft is visible in the dorsal and posterior part of layer A (arrowheads in Figs. 2Aa, b, Ea), but not in the ventral or anterior part. The lateral subdivision of layer A gradually disappears anteriorly (Figs. 2Ab, c, d, e), as the cleft exits the lateral edge of the LGB (i.e. convex surface of the three-dimensional C described below), between levels of Figures 2Ab and c. There are occasional gaps in the ventral part of layer C, especially medially (Fig. 2Ac) through which layers A1 and C1 come into close contact (Fig. 2Bc). MIN layer 1 becomes bigger anteriorly (Fig. 2A). Posteriorly, layer 3 is larger than layer 1. Due to an uneven distribution of labeled afferents, layer 3 appears bilaminar at some levels in this animal (Fig. 2Aa). Layer 3 is divided anteriorly into dorsal and ventral segments containing large soma (Figs. 2Ad,e).

To maintain the same orientation, drawings of the ipsilateral eye layers were flipped left to right in Figure 2B. Unlike layer A, no cleft subdividing layer A1 was identified. The ventral border of layer A1 often appears dentated, breaking the continuity of layer C, as best seen in Figure 2Bc. Layers 2 and 4 appear broken anteriorly into several segments, as best seen in Figure 2Be. The breakage points corresponded to zones containing few somata and weak label (Fig. 4I).

Layer A extended further laterally than A1 (compare Figs. 1A and B). This probably reflects the monocular representation, as pointed out in earlier studies in the cat (Guillery and Stelzner, 1970) and in the mink LGN (Guillery and Oberdorfer, 1977). The label in C2, however, was continuous. The lateral margin of layer A1 is roughly aligned with the breakage points in layers A and C (arrowheads in Figs. 2Ac, d and e).

Figure 2C is a summary section showing the laminar structure of the dog LGB combined from slices of the representative contralateral (Fig. 2Ad) and ipsilateral (Fig. 2Bd) layers. The zones filled with labeled afferents from the contralateral and ipsilateral eyes fit with one another fairly well at this level. Layer A is the largest layer of all. The MIN consists of four orderly alternating layers of the contralateral and ipsilateral layers. The arrow points to a small laminar gap, beyond which layers A1 and C1 are no longer present and the number of layers abruptly changes from 5 to 3. This transition obviously marks the outer limits of binocular vision. The transition forms a three-dimensional groove on the lateral surface of the LGB (convex surface of the three-dimensional C). Thus, the region lateral to this groove represents the monocular crescent.

We next show the LGB in parasagittal (Fig. 2D) and horizontal (Fig. 2E) sections. In Figure 2Da, layers C and

Fig. 2. Computer-generated 2D sections from the reconstructed 3D object. **A:** Representative sections of contralateral eye layers in the right MIN/LGN complex, posterior to anterior, selected from 79 slices. Each layer is color-coded according to the color-map in C. Five layers can be identified: layers A, C, C2 for the LGN, and layers 1, 3 for the MIN. Layer A is partially divided in posterior sections (a,b) into medial and lateral parts by a cleft (arrowheads in Figs. Aa,b). The lateral margin of layer A1, which defines the monocular segment, is roughly aligned with breaks in layers A and C (arrowheads in Figs. Ac,d and e) that presumably represent the optic disk. **B:** Representative sections of ipsilateral eye layers, posterior to anterior, selected among 68 slices. a–e: Sections made for the left side of the brain were flipped left to right to make the same orientation as in A. Four layers could be identified: A1, C1 for the LGN, and 2, 4 for the MIN. **C:** Representative section showing the laminar structure of the dog LGB, combined from sections of a contralateral (Fig. 2Ad) and ipsilateral (Fig. 2Bd) layers. MIN consists of four orderly alternating, contralateral and ipsilateral layers. The arrowhead points to the presumptive border of the monocular segment. **D:** Representative parasagittal sections of contralateral eye layers, lateral to medial. Ipsilateral eye layers are not shown. An arrowhead in panel a points to a cleft which divides layer A into medial and lateral subdivisions. **E:** Representative horizontal sections of contralateral eye layers, dorsal to ventral. Ipsilateral eye layers are not shown. In panel Ea, a cleft that divides layer A into medial and lateral subdivisions is indicated by an arrowhead. Figure orientation and calibration are shown to the left of panel C. The size of C is twice that of A or B. Note that the length of calibration bar for A,B, and C is slightly shorter than those for D and E, and that it is 2 mm for A and B, but 1 mm for C.

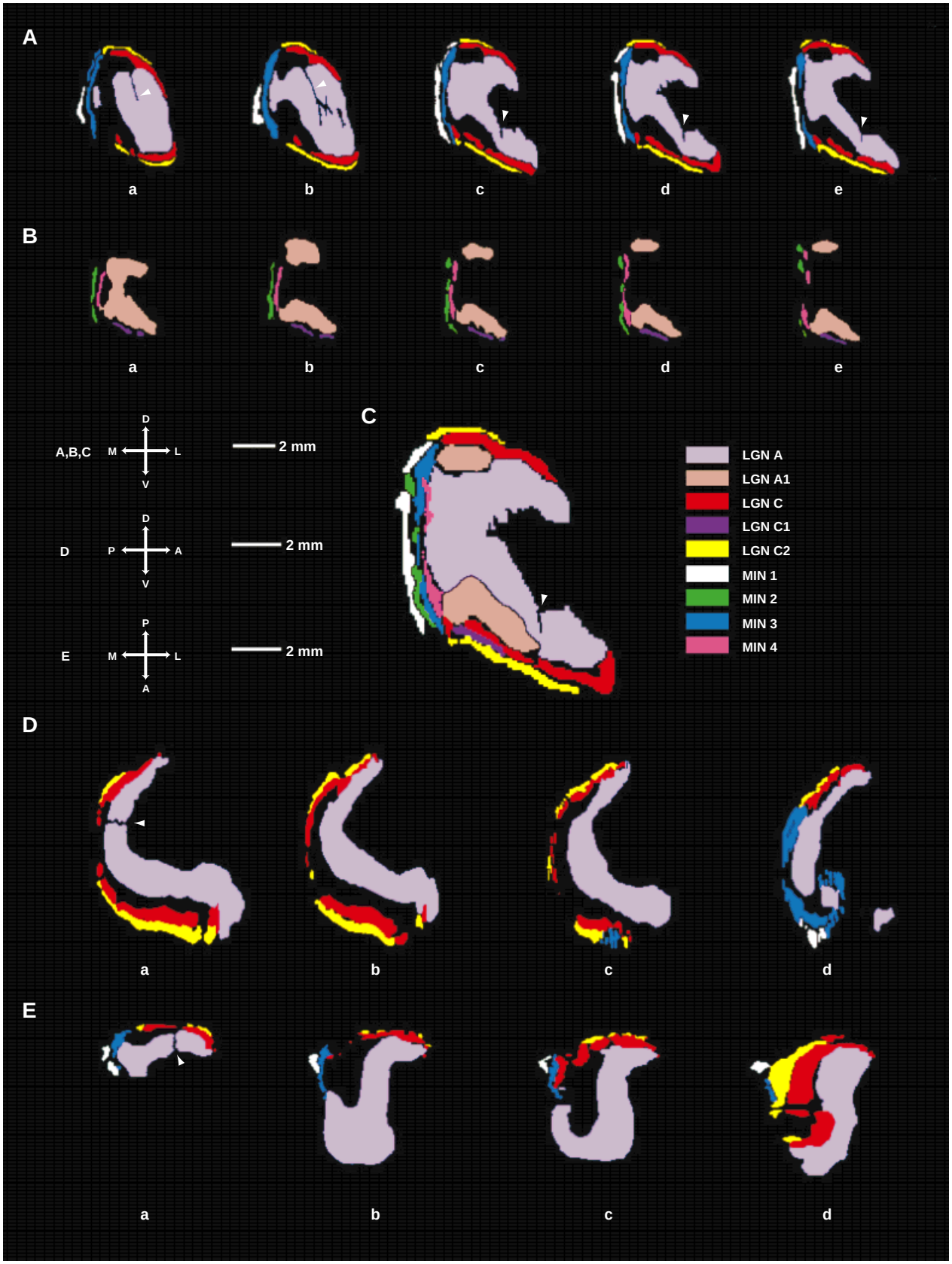
A
a
b
c
d
e
B
a
b
c
d
e
A,B,C
D
M
L
V
2 mm
D
D
P
A
V
2 mm
E
P
M
L
A
2 mm
C
LGN A
LGN A1
LGN C
LGN C1
LGN C2
MIN 1
MIN 2
MIN 3
MIN 4
D
a
b
c
d
E
a
b
c
d

Figure 2.

C2 are thin and discontinuous at the posterior pole of the complex, which was also confirmed in parasagittal sections of a third dog (*Sapsaree*), stained with cresyl violet. The break in layer A dividing medial and lateral subdivisions is visible in parasagittal and horizontal sections (arrowheads in Fig. 2Da and Fig. 2Ea). Since the break is oblique, it appears a line at the level of the parasagittal section shown in 2Da. The break in layer A in parasagittal section (Fig. 2Da) is presumably the optic disc representation that has been described in previous comparative studies (Kaas et al., 1973; Sanderson, 1974). The cleft in layer A (Fig. 2Aa, b) appears to be continuous with the three-dimensional groove formed by breakage points in layer A (Fig. 2Ac, d and e).

Three-Dimensional Views of the LGN/MIN Layers

Figure 3 shows three-dimensional view of the computer-reconstructed LGB for the contralateral (left) and ipsilateral (right) side. The combined complex appears like the letter C, with the convex part of the C directed posteriorly. The dorsal surface corresponds to layer A, which has a ventral groove running anteroposteriorly, as indicated by an arrow in 'LGN A.' This groove continues upward and medially at the posterior aspect. Layer A1 is shaped like the letter L, and fits in the ventral groove of layer A. Thus layer A1 is located underneath layer A at anterior levels, but it is medially located at the middle level of the complex, and at posterior levels, it dorsally caps layer A. The bottom part of layer A1 has an irregular surface, especially at posterior levels. These irregular protrusions invade the occasional discontinuities in layer C in two-dimensional sections (Figs. 1E,G, Fig. 2Bc). Layer C wraps around layer A1 ventroposteriorly. Thus, the contralateral layers A and C form a tunnel to be filled by layer A1. Layer C1 is located underneath layer C. Layer C2, in turn, wraps around layers C and C1 ventrally and posteriorly. Whereas layers A and A1 are continuous, layers C, C1, and C2 are somewhat discontinuous at the posterior pole of the complex. The three-dimensional shapes of the MIN layers can be described as torn plates with slight curvature.

Morphology of Soma in Each Layer

Once the zones filled with labeled afferents were associated with LGN/MIN layers (see Methods), the cytoarchitectonic characteristics of individual layers were examined. Figure 4 illustrates histological characteristics of the finally-determined LGN/MIN layers in representative counterstained sections, adjacent to HRP-reacted sections.

In posterior sections, a cleft in soma distribution was noticeable in the middle of layer A (arrow in Fig. 4A). The cleft was approximately 70 µm in width. It contained no somata and no labeled afferents. As mentioned above, this cleft divided layer A into medial (to the left in Fig. 4A) and lateral subdivisions. Compared with the lateral subdivision, the medial subdivision contained larger somata and had a higher density of labeled retinal afferents. Cell density was lower in the lateral subdivision, and it decreased laterally within the lateral subdivision. Soma size was variable in both medial and lateral subdivisions. Soma size in layer A1 was similar to that of layer A and evenly distributed (Fig. 4B). Layer C contained large round somata that were sparsely spaced (Fig. 4C). Layer C1 contained small somata sparsely distributed, and the density of labeled afferents was low, defining its border (Fig. 4C). Layer C2 had round medium-sized somata that were evenly distributed, and layer C3 had few somata, showing no labeled afferents from either retina (Fig. 4C).

Figure 4D was taken from the section adjacent to the one in Figure 2Ab, showing a ventral view of MIN layer 1. This layer contained the largest soma of all LGN/MIN layers (soma size in the long axis reaching up to 50 µm), and a high density of labeled afferents from the contralateral eye. Layer 2 contained spindle-shaped large-sized somata and a high density of labeled afferents from the ipsilateral eye (Fig. 4E). The ventral part of layer 3 contained large somata and a high density of label (Fig. 4F). Figure 4G shows a dorsal aspect of the contralateral side at a posterior level (roughly corresponding to the upper left aspect of Figure 1A). At this level, the labeled afferents were evenly distributed, making laminar borders difficult to define. However, as can be seen in this Nissl-stained section, there was a zone free of soma separating MIN layer 3 and LGN layer A, as indicated by an arrow. MIN layer 4 contained somata of various size, and was separated from LGN layer A1 by a zone free of somata (arrow in Fig. 4H). The middle portion of layer 4, which was separated from layer A by a zone free of somata (arrow), and which connected the dorsal and ventral parts of layer 4, contained few somata and weak labeled afferents from the ipsilateral eye (Fig. 4I). In general, middle parts of the MIN layers bridging the dorsal and ventral bulbs contained few somata and were characterized by a low density of labeled afferents.

The medial part of the contralateral side was often filled with continuously labeled afferents. In Figure 1E, for example, the zones filled with labeled afferents appeared continuous from the medial aspect of layers C and C2 to layer 3. However, in an adjacent counterstained section (Fig. 4J), a zone free of somata (indicated by two arrows) separated MIN layer 3 from the LGN. The distinction between layers C and C2 was aided by the large round somata in layer C.

Laminar Volumes

The volume of each LGN/MIN layer was obtained by summing voxels in each coronal section. Table 1 illustrates the results from one animal that showed stronger label. Since the zones labeled with retinal afferents roughly coincided with zones of somata, we believe the voxel counts closely reflect laminar volumes. The anteriormost 400 µm of the LGB in this animal, consisting of only layer A (see Fig 2E), was not processed for HRP. The volume of this region was estimated to be 0.47 mm^3 (1.18% of the total

Fig. 3. Three-dimensional views of the reconstructed LGB for the contralateral (left) and ipsilateral (right) side of the brain. The viewing angle for the complex on each side is indicated by the rectangular solid figures. P, posterior; L, lateral; V, ventral; D, dorsal faces of the rectangular blocks. The views of all LGN/MIN layers (ALL), LGN layers (middle), and MIN layers (bottom) are given in the same orientation. A cube below LGN C1 on the right side provides a calibration for both contralateral and ipsilateral sides. The combined complex appears as the letter C. The dorsal part of the C corresponds to layer A, which has a groove underneath running anteroposteriorly (arrow in LGN A). Layer A1 is located underneath layer A. The empty part of MIN layer 3 is due to the fact that the middle portion of this layer is elongated dorsoventrally, lacking in large soma and labeled afferents.

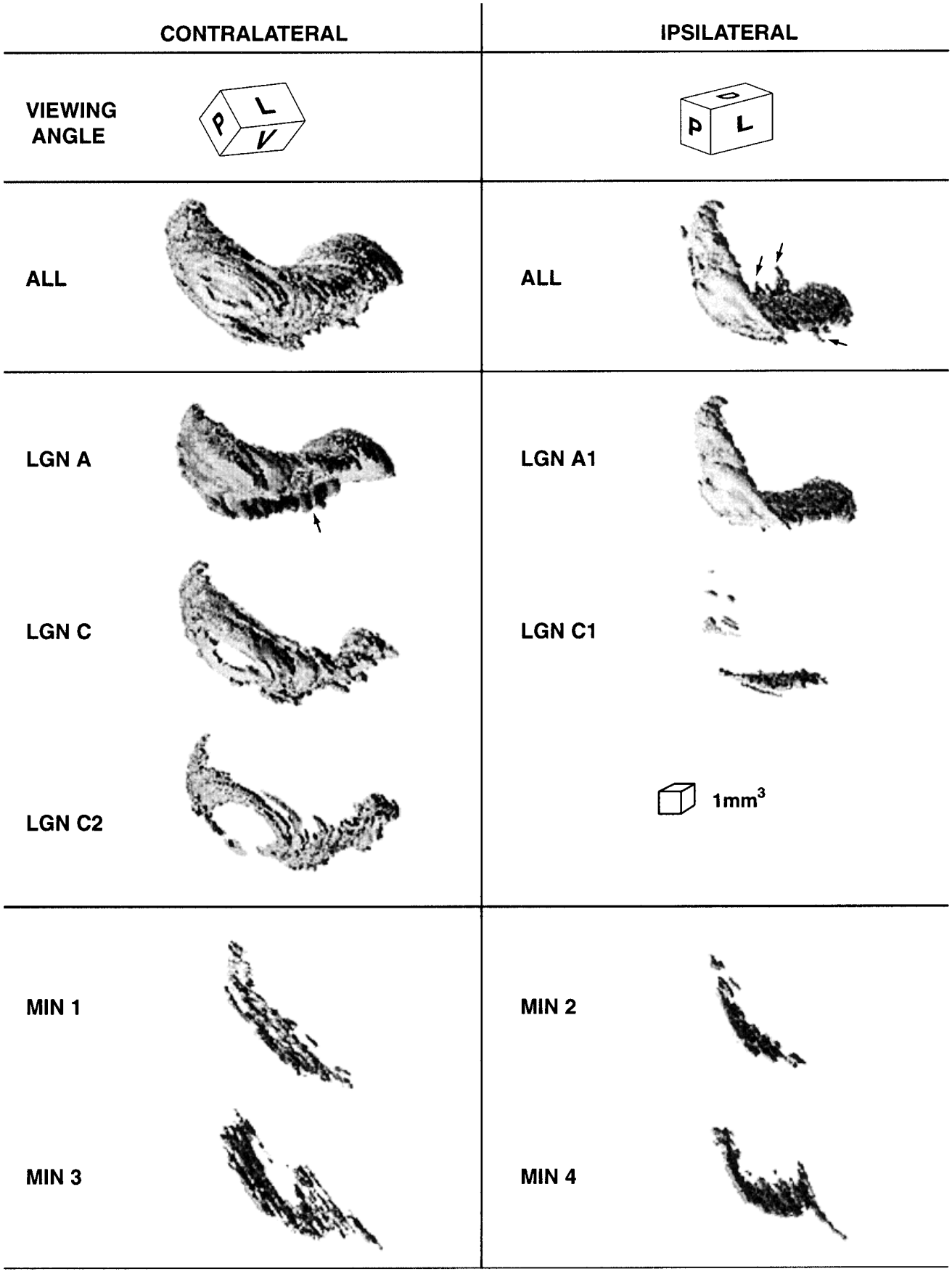
CONTRALATERAL
IPSILATERAL
VIEWING ANGLE
P
L
V
D
P
L
ALL
ALL
LGN A
LGN A1
LGN C
LGN C1
LGN C2
1mm3
MIN 1
MIN 2
MIN 3
MIN 4

Figure 3.

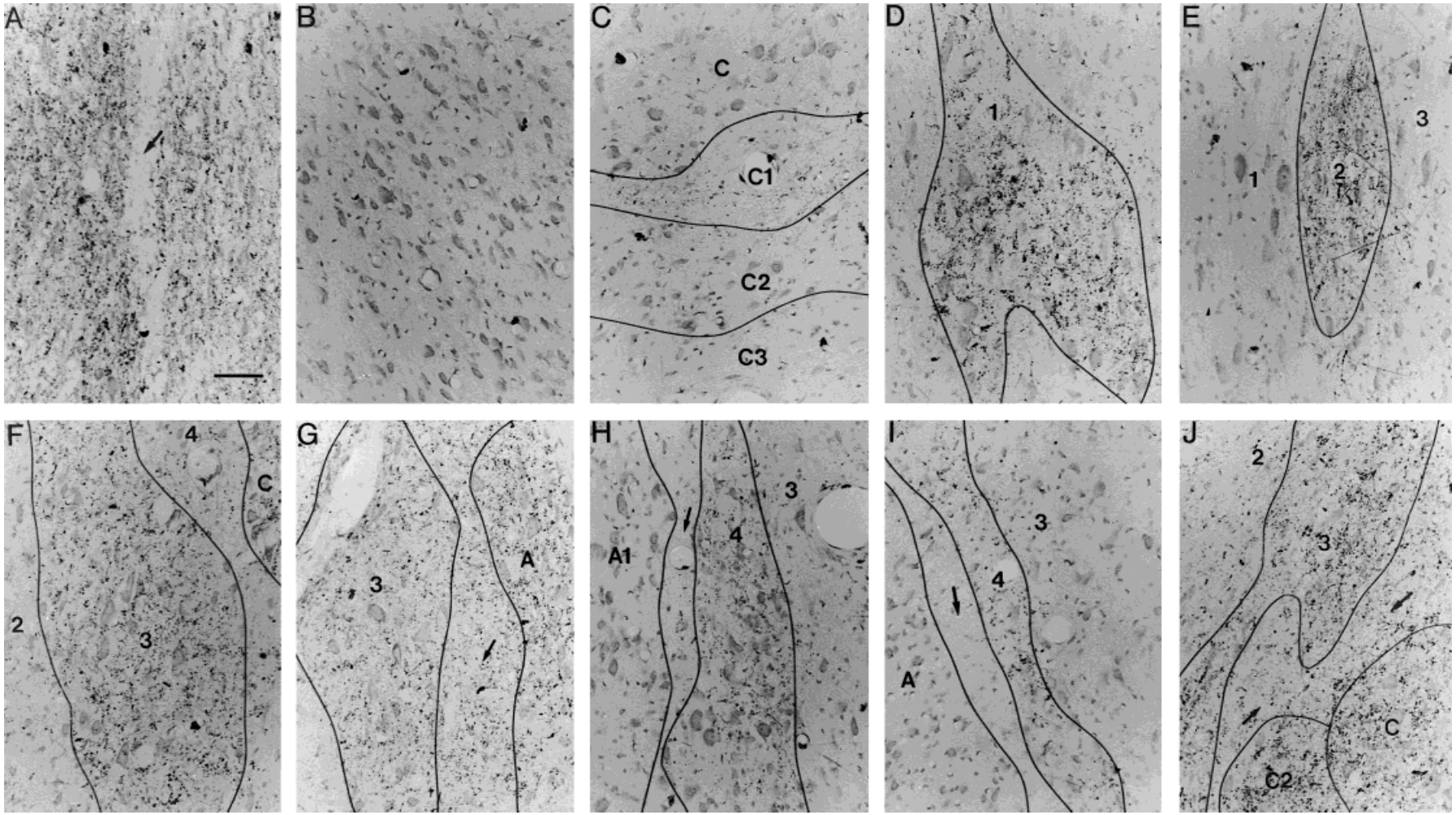

Fig. 4. Composite photomicrographs of representative coronal sections. These sections were processed for HRP and counterstained with neutral red, and viewed at ×200 with light-field illumination. The calibration bar in A corresponding to 100 µm, corrected for tissue shrinkage, applies to all panels except J. Dorsal is up for all panels. Dark granules are HRP-reaction product. **A:** Dorsal part of layer A contralateral to the injected eye. The arrow points to the cleft running up-down and dividing layer A into medial and lateral subdivisions. Medial is to the left. **B:** Types of soma in layer A1. They ranged from small to large size and evenly distributed. Medial is to the left. **C:** The LGN C layers. Layer C contained large round soma that were sparsely spaced. Layer C1 contained small soma sparsely distributed. Layer C2 had round medium-sized soma that were evenly distributed. Layer C3 had few soma and showed no labeled afferents from either retina. Medial is to the right. **D:** MIN layer 1, taken from the ventral most part in adjacent section to the one in Figure 2Ab. This layer contained the largest soma of all LGN/MIN layers. Medial is to the left. **E:** Ventral part of the MIN layer 2, corresponding to the zone labeled 2 in Figure 1D. This layer contained spindle-shaped large-sized soma and a high density of labeled afferents from the ipsilateral eye. Medial is to the left. **F:** Ventral part of MIN 3. Medial is to the left. **G:** Dorsal aspect of the contralateral side at posterior level (roughly corresponding to the left upper aspect of Figure 1A). A zone free of soma separating MIN layer 3 from LGN layers A and C is indicated by an arrow. Medial is to the left. **H:** Ventral aspect of MIN layer 4. A zone free of soma separating layer 4 from LGN layer A1 is indicated by an arrow. Medial is to the right. **I:** Middle portion of MIN layer 4 containing few soma and weak labeled afferents from the ipsilateral eye. An arrow indicates a zone free of somata separating the layer 4 from LGN layer A. In general, middle parts of the MIN layers containing strong label bridge the dorsal and ventral tiers. Medial is to the right. **J:** Medial aspect of the contralateral side shown in Figure 1E. The figure is rotated about 45 degrees to include layers C, C2, and 3. Medial is to the upper left corner. Dorsal is upper right. A zone free of soma (indicated by two arrows) separated MIN layer 3 from LGN. Distinguishing layers C and C2 was facilitated by the large and round soma in layer C.

TABLE 1. Volume of each LGN/MIN layer*

	Contralateral		Ipsilateral		Total
LGN	A	21.3	A1	7.6	
	C	5.6	C1	0.3	37.2
	C2	2.4			(93)
Subtotal		29.3		7.9	
MIN	1	0.9	2	0.3	
	3	1.0	4	0.4	2.6
					(7)
Subtotal		1.9		0.7	
Total		31.2		8.6	39.8
		(78)		(22)	(100)

*Laminar volumes in mm^3 were obtained by summing voxels in each coronal section. Each voxel corresponded to 0.0000504 mm^3 ($0.03 \times 0.03 \times 0.056$ mm, corrected for tissue shrinkage). Volume percentage is given in parentheses. Total volume of the LGB was 39.8 mm^3. The LGN constituted 93% and the MIN, 7% of the whole complex. Contralateral layers occupied 78%, and the ipsilateral, the remaining 22%.

volume) by interpolating the trend of areal decrease, and this is included in Table 1. The total volume of the dog LGB was 39.8 mm^3. The LGN constituted 93%, and the MIN 7% of the whole complex. Contralateral layers occupied 78%, and ipsilateral layers the remaining 22%. The calculation of these volume fractions was based on the assumption that no regions of the LGB receive binocular inputs. The MIN constituted a similar fraction of the entire LGB on the two sides of the brain, 8% on the ipsilateral side and 6% on the contralateral side. Within the LGN, the ipsilateral projection was mostly directed to layer A1 (96%), with the remainder going to layer C1 (4%). In comparison, layer A occupied 68% of the total contralateral projection to the LGN.

Laminar volumes of the cat LGN were estimated from figures of Sanderson (1971), and are compared to those of the dog in Table 2. Sanderson's figures did not distinguish subdivisions of the C layers or of the MIN, and his layer C probably included C3 which does not receive retinal input. Since our volume estimates for the dog LGN are based on retinal afferents, direct comparisons with layer C of cat are pointless. Overall, volumes of the whole LGB are similar in two species, but two differences are apparent. First, the relative volume of the MIN is smaller in the dog: the percentage of the canine MIN volume, relative to the combined volume of layers A, A1 and the MIN, was 8.3%, while that in the cat was 14.2%. Second, the ratio of contralateral to ipsilateral laminar volumes is much larger in the dog than in the cat: the ratio of layer A to layer A1 was 2.8 in the dog while that in the cat was 1.25.

DISCUSSION

The dorsal LGB of the carnivore has been known to consist of two subdivisions: the LGN and the MIN (Sanderson, 1974; Thuma, 1928). Both anatomical and electrophysiological studies indicated that these nuclei receive inputs from both eyes (Guillery et al., 1980; Hayhow, 1958; Lee et al., 1984; Morimoto et al., 1984; Sanderson, 1971), and project to various areas of the visual cortex (Birnbacher and Albus, 1987; Hollander and Vanegas, 1977; Humphrey et al., 1985; Niimi et al., 1981; Raczkowski and Rosenquist, 1983; Tong and Spear, 1986). Compared to the cat, the relative volume of ipsilateral layers was small (Tables 1 and 2). This perhaps is related to the extent of the partial decussation and direction of the optical axis; the dog has more lateral facing eyes, and thus a smaller binocular field compared to the cat.

One new finding is that the dog MIN consists of four orderly interdigitating layers; two contralateral layers (layers 1 and 3) and two ipsilateral layers (layers 2 and 4). Morimoto et al. (1984) reported two MIN layers based on HRP-materials. However, in their Figures 6d,e, one can see possible indications of the bilaminar nature of the contralateral and ipsilateral MIN layers. With two-dimensional sections alone, however, it was probably difficult to identify unambiguously the MIN layers. Accordingly, Guillery et al. (1980) expressed this ambiguity by suggesting that MIN layer 3 of the cat might be considered an extension of layer C. Similarly, in the present study HRP-reacted sections alone were insufficient to determine whether the zones corresponding to MIN layers 3 and 4 were independent structures or continuations of the ventral LGN layers C and C1. However, from the morphological characteristic of three-dimensional reconstructions of the zones filled with labeled retinal afferents, separation and singleness of each layer could be appreciated. The three-dimensional models, combined with cytoarchitectonic characteristics such as the size or density of somata associated with labeled afferents, definitively resolved the ambiguity in laminar determination, and we believe that all four MIN layers are distinct from the LGN layers. The HRP histochemistry method, when combined with computer reconstruction, has proved to be an extremely efficient method for characterizing the laminar structure, using a small number of animals. General patterns of lamination in our breed (*Sapsaree*) were almost identical with those of unknown or mixed breeds used in previous studies (Howard and Breazile, 1973; Morimoto et al., 1984; Rioch, 1929). However, we cannot exclude the possibility that interbreed differences in cytoarchitecture of the LGN/MIN exist, and that they account for the new MIN layers found in this study.

The MIN appears to be specialized for nocturnal vision in the cat. The cat MIN almost exclusively represents a region of retina roughly coincident with the reflective tapetum, mainly mapping the lower visual field (Lee et al., 1984). The tapetum, a reflective layer behind the retina found in almost all carnivores, enhances night vision by allowing the photoreceptor a second chance at absorbing light reflected by this mirror-like structure. The spatial coincidence between the tapetum and the MIN in the cat suggests roles of the MIN for dim-light vision. This is supported by the evidence that, compared to their LGN counterparts, cells of the MIN have lower luminance threshold at low adaptation levels: for stimuli with low spatial frequency, MIN cells continue to respond until the adaptation level decreases 1 log unit below the limit for LGN cells (Lee et al., 1992). It is unknown if the dog MIN has a similar role in dim-light vision. This study was undertaken to guide further investigations into possible functions of canine MIN. The volume of the dog MIN relative to the LGN is smaller than the cat MIN (Table 2), suggesting that MIN cells of the dog might have bigger receptive fields than their feline counterparts, resulting from more retinogeniculate convergence.

The well-developed lamination of the dog MIN might reflect the importance of nocturnal vision in this creature,

TABLE 2. Comparison of laminar volumes between the dog and the cat*

	A	A1	C	MIN	ALL
Dog	21.3 (53.5)	7.6 (19.1)	8.3 (20.9)	2.6 (6.5)	39.8 (100)
Cat	13.48 (35.5)	10.75 (28.3)	9.76 (25.7)	4.0 (10.5)	37.99 (100)

*Laminar volumes of the cat were estimated from figures of Sanderson (1971). Numbers are in mm^3 and numbers in parentheses are volume percentage. Overall, volumes of the whole LGB are similar in the two species. Compared with the cat, relative volume of the MIN, and ratio of layer A1 (ipsilateral) to layer A (contralateral) are lower in the dog. See text for details.

as documented by dog breeders, and supported by the fact that the wolf, the dog's wild relative, make most of its kills at night. The dog's optical system appears to be optimized for dark sensitivity. The threshold of light for vision in dogs seems to be higher than that for cats, but they can analyze the intensity of low-level illumination excellently (Duke-Elder, 1958). The central 25 degrees of the dog retina consists mostly of rods (Kemp and Jacobson, 1992). The tapetal cell-like melanocytes distribute over most of the dog's fundus as in the cat (Chijiiwa et al., 1990). We examined the spatial distribution of the tapetum of the dogs used in the present study, and found that it appeared similar to that of the cat, strongly biased toward lower visual fields. In dogs, the visual streak is located within the tapetal retina (Hebel, 1976). This suggests that the dog's central vision may be enhanced in dim light at the expense of degradation of resolution by light scattered from the tapetum (Miller and Murphy, 1995). Furthermore, the shape of the dog's eyeball is considerably flatter anteroposteriorly, unlike the round eyeball of the cat. The mean axial diameter of the eyeball of the dogs used in this study was approximately 18 mm whereas the mean radial diameter was 21 mm. The shorter axial length inevitably reduces the size of retinal image and increases luminance per unit retinal area, presumably enhancing dim-light sensitivity.

The retinotopic organization of the dog LGB is unknown. Lee et al.(1984) described the retinotopic organization of the cat MIN. The vertical meridian is represented along the border between LGN and MIN. Within MIN layers 1 and 2 of the cat, the contralateral visual hemifield is systematically represented medially. Layer 3 of the cat represents the ipsilateral hemifield through the contralateral eye, as shown by anatomical (Guillery et al., 1980) and physiological (Lee et al., 1984) studies. Whereas the LGN represents the ipsilateral hemifield to a limited extent, 1–3 degrees of so-called nasotemporal overlap, the extent of the ipsilateral visual field represented in the cat MIN is almost 30 degrees (Lee et al., 1984). The quadrilaminar organization of the dog MIN raises several possibilities. First, layer 4 may represent the ipsilateral hemifield, like layer 3 of the cat, but through the ipsilateral eye. If so, MIN layers 3 and 4 could provide an independent binocular vision for the ipsilateral hemifield that might subserve a coarse stereopsis in the dog. Second, since MIN layers 3 and 4 layers are located near the border between the MIN and LGN, where the vertical meridian is mapped in the cat, they may represent a relatively more central region of contralateral visual space, and layers 1 and 2 a more peripheral zone via the two eye. Third, the two contralateral and two ipsilateral MIN layers may reflect the segregation of ON- and OFF-center cells, as has been shown in sublayers of the LGN in the mink (LeVay and McConnell, 1982), in the tree shrew (Conway et al., 1980), and in the ferret (Stryker and Zahs, 1983). In any case, the MIN layers of the dog are thinly staggered plates and the mediolateral extent of each layer is considerably thinner (about 300 μm) than that of the cat [compare Figure 2C and Figure 6 of Lee et al. (1984)]. This undercuts systematic retinotopy in mediolateral dimension across the border between the LGN and the MIN, unlike the cat. The precise retinotopy of the dog LGN/MIN will need to be understood for a firm comparison of its role as a nocturnal specialization with that of the cat LGN/MIN.

Layer A has been shown to be sublaminated to varying degrees in several carnivores (Sanderson, 1974). The division of the dog layer A into medial and lateral sublamina was partial; at anterior and ventral aspects, layer A was undivided. If the functional segregation within the layer A in the dog matches that in the ferret described by Stryker and Zahs (1983), the medial subdivision of the dog layer A would consist of OFF-center cells responding to decreases in light intensity, whereas the lateral subdivision would consist of ON-center cells. However, we think that the cleft in layer A is more likely to be the representation of the optic disc for two reasons. First, the cleft in layer A exited the dorsolateral surface of the LGB, continuing to the three-dimensional groove formed by the margin of the presumptive border of the monocular crescent. Second, the subdivision of layer A (Fig. 2Aa,b) was found in posterior coronal sections (Fig. 2Aa,b), which, if the overall retinotopic organization is similar to that of the cat, maps the lower retina, including the optic disk (Sanderson, 1971). Thus, it appears that the subdivision medial to the cleft represents the binocular visual field, whereas the lateral subdivision represents the monocular field. The optic disc representation (the cleft in layer A) constitutes a part of the boundary of the monocular representation (the three-dimensional groove).

ACKNOWLEDGMENTS

The dogs used in this study were kindly supplied by Dr. JiHong Ha. We thank Dr. Joseph Malpeli for his constructive comments on the manuscript. This research was supported by the Biotech-2000 program of the Korea Ministry of Science and Technology.

LITERATURE CITED

Birnbacher D, Albus K. 1987. Divergence of single axons in afferent projections to the cat's visual cortical areas 17, 18, and 19: a parametric study. J Comp Neurol 261:543–561.

Chadzypanagiotis D, Narkiewicz O, Sernicki A. 1968. The interlaminar nuclei of the lateral geniculate body in the dog. Folia Morphol 27:432–438.

Chijiiwa T, Ishibashi T, Inomata H. 1990. Histological study of choroidal melanocytes in animals with tapetum lucidum cellulosum. Graefes Arch Clin Exp Ophthalmol 228:161–168.

Conway J, Schiller PH, Mistler L. 1980. Functional organization of the tree shrew lateral geniculate nucleus. Soc Neurosci Abstr 6:583.

Duke-Elder S. 1958. System of ophthalmology. In The eye in evolution. St. Louis: CV Mosby; p 605–706.

Guillery RW, Oberdorfer MD. 1977. A study of fine and coarse retino-fugal axons terminating in the geniculate C laminae and in the medial interlaminar nucleus of the mink. J Comp Neurol 176:515–526.

Guillery RW, Stelzner DJ. 1970. The differential effects of unilateral lid closure upon the monocular and binocular segments of the dorsal lateral geniculate nucleus in the cat. J Comp Neurol 139:413–421.

Guillery RW, Geisert Jr EE, Polley EH, Mason CA. 1980. An analysis of the retinal afferents to the cat's medial interlaminar nucleus and to its rostral thalamic extension, the "geniculate wing." J Comp Neurol 194:117–142.

Hayhow WR. 1958. The cytoarchitecture of the lateral geniculate body in the cat in relation to the distribution of the crossed and uncrossed optic fibers. J Comp Neurol 110:1–64.

Hebel R. 1976. Distribution of retinal ganglion cells in 5 mammalian species (pig, sheep, ox, horse, dog). Anat. Embryol (Berl) 150:45–51.

Hollander H, Vanegas H. 1977. The projection from the lateral geniculate nucleus onto the visual cortex in the cat. A quantitative study with horseradish-peroxidase. J Comp Neurol 173:519–536.

Howard DR, Breazile JE. 1973. Optic fiber projections to dorsal lateral geniculate nucleus in the dog. Am J Vet Res 34:419–424.

Humphrey AL, Sur M, Uhlrich DJ, Sherman SM. 1985. Termination patterns of individual X- and Y-cell axons in the visual cortex of the cat: projections to area 18, to the 17/18 border region, and to both areas 17 and 18. J Comp Neurol 233:190–212.

Kaas JH, Guillery RW, Allman JM. 1973. Discontinuities in the dorsal lateral geniculate nucleus corresponding to the optic disc: a comparative study. J Comp Neurol 147:163–180.

Kemp CM, Jacobson SG. 1992. Rhodopsin levels in the central retinas of normal miniature poodles and those with progressive rod-cone degeneration. Exp Eye Res 54:947–956.

Lee C, Malpeli JG, Schwark HD, Weyand TG. 1984. Cat medial interlaminar nucleus: retinotopy, relation to tapetum and implications for scotopic vision. J Neurophysiol 52:848–869.

Lee D, Lee C, Malpeli JG. 1992. Acuity-sensitivity trade-offs of X and Y cells in the cat lateral geniculate complex: role of the medial interlaminar nucleus in scotopic vision. J Neurophysiol 68:1235–1247.

LeVay S, McConnell SK. 1982. ON and OFF layers in the lateral geniculate nucleus of the mink. Nature 300:350–351.

Mesulam M-M. 1982. A tetramethylbenzidine method. In Mesulam MM, editor. Tracing neural connections with horseradish peroxidase Chichester: John Wiley and Sons; p 127–130.

Miller PE, Murphy CJ. 1995. Vision in dogs. J Am Vet Med Assoc 207:1623–1634.

Morimoto M, Kubota T, Miyahara H, Kanaseki T. 1984. The laminar structures and axon terminals of the retinal fibers in the dorsal lateral geniculate nucleus of the dog. Fukuoka Igaku Zasshi 75:633–644.

Niimi K, Matsuoka H, Yamazaki Y, Matsumoto H. 1981. Thalamic afferents to the visual cortex in the cat studied by retrograde axonal transport of horseradish peroxidase. Brain Behav Evol 18:114–139.

Raczkowski D, Rosenquist AC. 1983. Connections of the multiple visual cortical areas with the lateral posterior-pulvinar complex and adjacent thalamic nuclei in the cat. J Neurosci 3:1912–1942.

Rioch DMK. 1929. Studies on the diencephalon of the carnivora. Part I. The nuclear configuration of the thalamus, epithalamus, and hypothalamus of the dog and cat. J Comp Neurol 49:1–119.

Sanderson KJ. 1971. The projection of the visual field to the lateral geniculate and medial interlaminar nuclei in the cat. J Comp Neurol 143:101–118.

Sanderson KJ. 1974. Lamination of the dorsal lateral geniculate nucleus in carnivores of the weasel (Mustelidae), raccoon (Procyonidae) and fox (Canidae) families. J Comp Neurol 153:239–266.

Stryker MP, Zahs KR. 1983. ON and OFF sublaminae in the lateral geniculate nucleus of the ferret. J Neurosci 3:1943–1951.

Thuma BD. 1928. Studies on the diencephalon of the cat. Part I. The cytoarchitecture of the corpus geniculatum laterale. J Comp Neurol 46:173–199.

Tong L, Spear PD. 1986. Single thalamic neurons project to both lateral suprasylvian visual cortex and area 17: a retrograde fluorescent double-labeling study. J Comp Neurol 246:254–264.